Accepted Manuscript

Half-sandwich d^6 metal complexes comprising of 2-substituted-1,8-napthyridine ligands with unexpected bonding modes: Synthesis, structural and anti-cancer studies

Sanjay Adhikari, Omar Hussain, Roger M. Phillips, Mohan Rao Kollipara

PII: S0022-328X(17)30660-5

DOI: 10.1016/j.jorganchem.2017.11.011

Reference: JOM 20176

To appear in: *Journal of Organometallic Chemistry*

Received Date: 12 October 2017

Revised Date: 9 November 2017

Accepted Date: 10 November 2017

Please cite this article as: S. Adhikari, O. Hussain, R.M. Phillips, M.R. Kollipara, Half-sandwich d^6 metal complexes comprising of 2-substituted-1,8-napthyridine ligands with unexpected bonding modes: Synthesis, structural and anti-cancer studies, *Journal of Organometallic Chemistry* (2017), doi: 10.1016/j.jorganchem.2017.11.011.

Half-sandwich d^6 metal complexes comprising of 2-substituted-1,8-napthyridine ligands with unexpected bonding modes: Synthesis, structural and anti-cancer studies

Sanjay Adhikari[a], Omar Hussain[b], Roger M Phillips[b], Mohan Rao Kollipara[a*]

[a]Centre for Advanced Studies in Chemistry, North-Eastern Hill University, Shillong 793022, India. E-mail: mohanrao59@gmail.com

[b]Department of Pharmacy, School of Applied Sciences, University of Huddersfield, Huddersfield HD1 3DH, UK

12 **Graphical abstract**

13

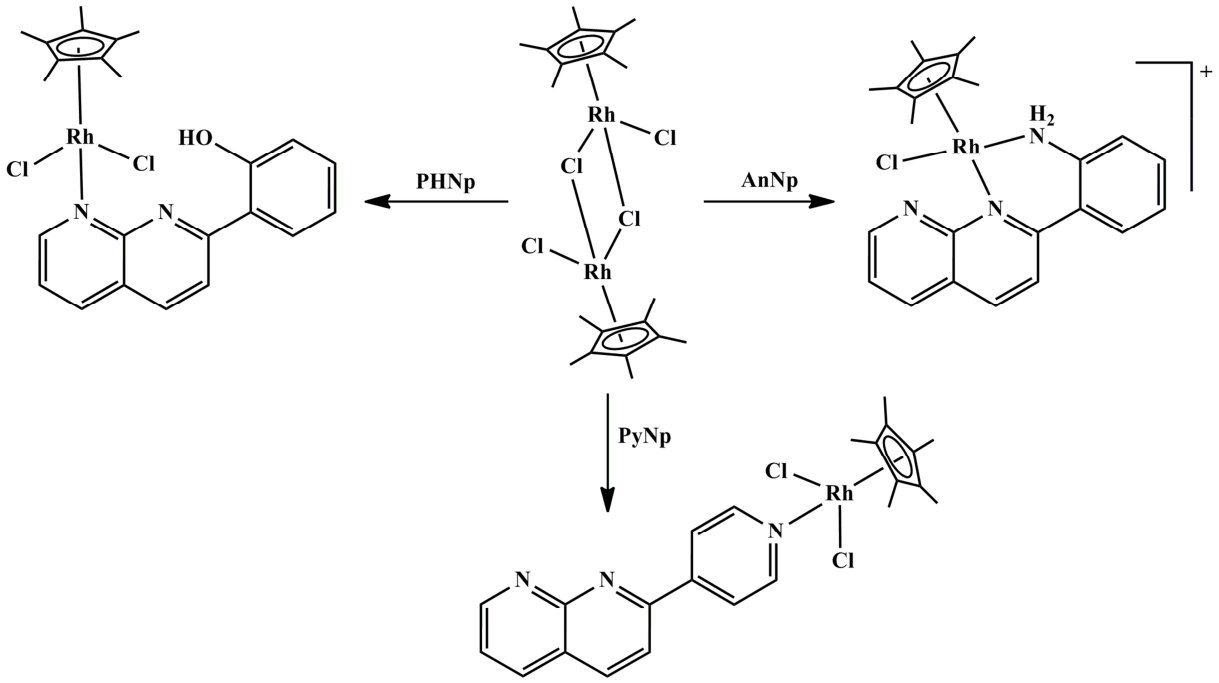

14

Abstract

The Friedländer condensation reaction between 2-aminonicotinealdehyde and acetophenone derivatives in presence of potassium hydroxide yielded 2-substituted-1,8-napthyridine derivatives *viz.* 2-(1,8-napthyridin-2-yl)phenol (PHNp), 2-(1,8-napthyridin-2-yl)aniline (AnNp) and 2-(pyridine-4-yl)-1,8-napthyridine (PyNp). Treatment of the chloro-bridged dimers $[(arene)MCl_2]_2$ [arene = *p*-cymene, Cp*; M = Ru, Rh and Ir] with two equivalents of napthyridine ligands (PHNp, AnNp and PyNp) allowed the formation of mononuclear napthyridine complexes having formula $[(arene)M(PHNp)Cl_2]$ (**1**-**3**), $[(arene)M(AnNp)Cl]PF_6$ (**4**-**6**) and $[(arene)M(PyNp)Cl_2]$ (**7**-**9**). These napthyridine compounds were isolated as neutral and cationic complexes which were further characterized by analytical and spectroscopic techniques. The molecular structures of some of the respective napthyridine complexes were established by carrying out the single crystal X-ray analysis. Single crystal X-ray studies revealed the coordination of the napthyridine ligands to the metal center wherein AnNp ligand coordinated metal in a bidentate chelating NN´ manner and PHNp and PyNp ligand coordinated metal in a monodentate fashion. In case of PHNp complexes the coordination occurs through napthyridine nitrogen N(1) whereas in case of PyNp complexes the coordination takes place through pyridine nitrogen N(1). These napthyridine complexes possessed cytotoxicity against HCT-116 (human colorectal cancer) and MIA-PaCa-2 (pancreatic carcinoma) cancer cell lines as compared to non-cancer cell line ARPE-19.

Keywords: Ruthenium, rhodium, iridium, napthyridine's, cytotoxicity

Introduction

Arene ruthenium complexes are a well-known class of organometallic compounds generally referred to as half-sandwich complexes having potential applications in many arenas [1]. These organometallic compounds have been found to possess clinical as well as industrial applications [2]. Ruthenium complexes have also displayed remarkable activity in medicinal chemistry and these complexes have the potential to act as metal based anti-cancer drugs [3, 4]. Two such complexes in particular namely $[Ru(\eta^6\text{-arene})Cl(en)]^+$ (en = ethylenediamine) and $[Ru(cymene)Cl_2(PTA)]$, known as RAPTA-C (PTA = 1,3,5-triaza-7-phosphaadamantane), have been found to possess excellent cytotoxic and anti-cancer activity both *in vitro* and *in vivo* including activity against cisplatin resistant cancer cells [5, 6]. Analogous to arene ruthenium complexes, Cp* rhodium and Cp* iridium complexes are also being studied as an alternative to platinum based drugs because of the inert facial co-ligand Cp* which is expected to offer several advantages such as water solubility and lability [7]. These complexes also serve as catalysts for various organic transformations such as hydrogenation and C-H activation [8, 9].

1,8-napthyridines represents an important class of ligands containing two fused pyridine rings and whose structure is closely related to bipyridines and phenanthrolines. These ligands possess several donor sites thus allowing them to act as monodentate, bidentate chelating and bridging coordinating ligand [10]. Substitution of an appropriate donor groups such as pyridyl, thiazolyl, furyl and pyrrole at the 2-position of 1,8-napthyridine provides a ligand, which can coordinate metal with the substituted ring in addition to the napthyridine ring [11]. The napthyridine ligands acts as a bridge to communicate between the two metal centers to come close to each other and which is expected to alter the bonding magnetic or energy transfer interactions. In cases where the donor groups attached at the 2-position of the napthyridine ring were substituted phenyl (F and OMe) and N-methyl pyrrole groups, interesting coordinating

chemistry has been observed for diruthenium complexes [12]. Despite having a rich diversified chemistry of napthyridine metal complexes, it is noteworthy that only a few half-sandwich platinum group metal napthyridine complexes have been reported to date [10, 13]. Based on the reactivity and different bonding modes of napthyridine ligands we anticipated that what would be the outcome if we substitute donor group such as phenol, aniline and pyridine at the 2-position of the napthyridine ring. We assumed that the formed ligand would display distinctly unusual bonding modes and we have therefore explored this possibility in our present work. Ligands used in the present study are 2-(1,8-napthyridin-2-yl)phenol (PHNp), 2-(1,8-napthyridin-2-yl)aniline (AnNp) and 2-(pyridine-4-yl)-1,8-napthyridine (PyNp). To the best of our knowledge the coordination chemistry of these ligands has not been explored previously.

Herein, we report the synthesis and anti-cancer studies of ruthenium, rhodium and iridium half-sandwich complexes bearing phenol, aniline and 4-pyridyl groups substituted at 2-position of 1,8-napthyridine moiety.

Experimental

Physical methods and materials

The reagents used were of commercial quality and used without further purification. Metal chloride's $RuCl_3.nH_2O$, $RhCl_3.nH_2O$ and $IrCl_3.nH_2O$ were purchased from Arora Matthey Limited. α-phellandrene, pentamethylcyclopentadiene and 2´-hydroxyacetophenone were purchased from Sigma-Aldrich. 2-aminonicotinaldehyde and 4-acetyl pyridine were obtained from Alfa Aesar and 2´-aminoacetophenone was obtained from Spectrochem. The solvents were dried and distilled prior to use according to standard procedures [14]. Precursor metal complexes $[(p\text{-cymene})RuCl_2]_2$ and $[Cp^*MCl_2]_2$ (M = Rh/Ir) were prepared according to the published procedures [15, 16]. ^1H and ^{13}C NMR spectra were recorded on a Bruker Advance II 400 MHz

spectrometer using $CDCl_3$ and DMSO-d_6 as solvents; chemical shifts were referenced to TMS. Infrared spectra (KBr pellets; 400-4000 cm^{-1}) were recorded on a Perkin-Elmer 983 spectrophotometer. Mass spectra were obtained from Waters ZQ 4000 mass spectrometer by ESI method using acetonitrile as solvent. Elemental analyses of the complexes were carried out on a Perkin-Elmer 2400 CHN/S analyzer.

Structure determination by X-ray crystallography

Solvent diffusion method was used for growing single crystals of compounds by layering solutions of the compounds in dichloromethane or chloroform with a fourfold excess of hexane and allowing them to stand undisturbed for one week. Suitable single crystal of compounds were chosen and glued onto the tip of glass fiber which was centered in the X-ray beam. The data for the complexes was collected on an Oxford Diffraction Xcalibur Eos Gemini diffractometer using graphite monochromated Mo-Kα radiation (λ = 0.71073 Å). The strategy for the data collection was evaluated using the CrysAlisPro CCD software. Crystal data were collected by standard ''phi–omega scan'' techniques and were scaled and reduced using CrysAlisPro RED software. The structures were solved by direct methods using SHELXS-97 and refined by full-matrix least squares with SHELXL-97 refining on F^2 [17, 18]. The positions of all the atoms were obtained by direct methods. Metal atoms in the complex were located from the E-maps and all non-hydrogen atoms were refined anisotropically by full-matrix least-squares. Hydrogen atoms were placed in geometrically idealized positions and constrained to ride on their parent atoms with C---H distances in the range 0.95-1.00 Angstrom. Isotropic thermal parameters U_{eq} were fixed such that they were $1.2U_{eq}$ of their parent atom Ueq for CH's and $1.5U_{eq}$ of their parent atom U_{eq} in case of methyl groups. Crystallographic and structure refinement parameters for the complexes

104 are summarized in Table 1 and selected bond lengths and bond angles are presented in Table 2.
105 Figures 1-5 were drawn with ORTEP3 program [19].

106 The crystal structure of complex (**4**) contains disordered DCM molecule. Crystal
107 structure of complexes (**8** and **9**) contains $CHCl_3$ molecule in their solved structure.

108 ***Cell line testing***

109 The biological importance of the naphthyridines prompted us to study the cytotoxic
110 activity of the synthesized napthyridine ligands and complexes. The cytotoxicity was tested
111 against the HCT-116 colorectal carcinoma and MIA-PaCa-2 pancreatic carcinoma cell lines with
112 the IC_{50} result shown in Table 3. Both cell lines were originally purchased from the American
113 Type Culture Collection (ATCC) and all other reagents were purchased from Sigma Aldrich Co.
114 Ltd (Dorset, UK) unless otherwise stated. The ARPE-19 cell line which is a non-cancer, human
115 epithelial cell line derived from the retina and this was also obtained from ATCC. Cytotoxicity
116 of ligands and compounds were evaluated using the standard MTT 3-(4,5-Dimethylthiazol-2-yl)-
117 2,5-diphenyltetrazolium bromide cellular viability assay as follows. Cells were inoculated into
118 96 well plates at 1.5 x 10^3 cells per well and incubated at 37 $^{\circ}$C in an atmosphere of 5% CO_2
119 prior to drug exposure. The napthyridine ligands (Scheme 1) and complexes (**1**-**9**) (Scheme 2)
120 were all dissolved in DMSO at a concentration of 25 mM and diluted further with medium to
121 obtain drug solutions ranging from 0.5 to 150 μM. Cisplatin was dissolved in phosphate buffered
122 saline at a stock concentration of 25 mM. The final DMSO concentration was 0.2% (v/v), which
123 is nontoxic to cells. Cells were exposed to drug for 96 hours and cell survival was determined
124 using the MTT assay [20, 21]. Following drug exposure, 20 μL of MTT (0.5 mg/ml) in
125 phosphate buffered saline was added to each well and it was further incubated at 37 $^{\circ}$C for 4
126 hours in an atmosphere of 5% CO_2. The solution was then removed and the formed formazan

crystals was dissolved in 150 µM DMSO and the absorbance of the solution was recorded at 550 nm using an ELISA spectrophotometer. Percentage cell survival was calculated by dividing the true absorbance of treated cell by the true absorbance for controls (exposed to 0.2% DMSO). The IC_{50} values were determined from plots of % survival against drug concentration. Each experiment was repeated three times and a mean value obtained and stated as IC_{50} (µM) ± SD.

Synthesis of 2-substituted-1,8-napthyridine ligands

The ligands 2-(1,8-napthyridin-2-yl)phenol (PHNp), 2-(1,8-napthyridin-2-yl)aniline (AnNp) and 2-(pyridine-4-yl)-1,8-napthyridine (PyNp) were synthesized according to Friedländer condensation (Scheme 1) [22]. Herein a detailed procedure is provided only for 2-(1,8-napthyridin-2-yl)phenol (L1). A stirred solution of 2´-hydroxy acetophenone (408 mg, 3 mmol), 2-aminonicotinealdehyde (366 mg, 3 mmol) and KOH (336 mg, 6 mmol) in 50% aqueous methanol (10 mL) was heated to 60 °C overnight. The reaction mixture was quenched by the addition of water (20 mL) and the resulting precipitate was isolated by filtration. The crude product was washed with water, dried in vacuum and collected.

2-(1,8-napthyridin-2-yl)phenol (PHNp)

Color: Orange crystals; Yield: 82 %; IR (KBr, cm^{-1}): 3521(b), 3224(m), 2961(m), 2870(w), 1644(s), 1469(m), 1358(m); ^{1}H NMR (400 MHz, $CDCl_3$): δ = 14.7 (s, 1H, OH), 8.26 (d, 1H, *J* = 12 Hz), 8.15 (d, 1H, *J* = 8 Hz), 8.08 (d, 1H, *J* = 8 Hz), 7.90 (d, 1H, *J* = 8 Hz), 7.43-7.46 (m, 1H), 7.31-7.34 (m, 1H), 7.24 (d, 1H, *J* = 8 Hz), 7.06 (d, 1H, *J* = 8 Hz), 6.88-6.92 (m, 1H); Anal. Calc for $C_{14}H_{10}N_2O$ (222.24); C, 75.66; H, 4.54; N, 12.60. Found: C, 75.76; H, 4.67; N, 12.73 %.

2-(1,8-napthyridin-2-yl)aniline (AnNp)

Color: Yellow crystals; Yield: 86 %; IR (KBr, cm^{-1}): 3402(s), 3293(m), 3058(w), 2922(w), 1611(s), 1566(m), 1541(m), 1499(m), 1257(m); ^{1}H NMR (400 MHz, DMSO-d_6): δ = 8.84 (dd,

1H, *J* = 4 and 4 Hz), 8.28 (d, 1H, *J* = 8 Hz), 8.25 (dd, 1H, *J* = 4 and 4 Hz), 8.00 (d, 1H, *J* = 8 Hz), 7.70 (d, 1H, *J* = 8Hz), 7.38-7.41 (m, 1H), 7.34 (s, 2H, NH_2), 6.98 (t, 1H, *J* = 8 Hz), 6.65 (d, 1H, *J* = 8 Hz), 6.46 (t, 1H, *J* = 8 Hz); Anal. Calc for $C_{14}H_{11}N_3$ (221.25); C, 76.00; H, 5.01; N, 18.99. Found: C, 76.09; H, 5.12; N, 19.08 %.

2-(pyridine-4-yl)-1,8-napthyridine (PyNp)

Color: White powder; Yield: 65 %; IR (KBr, cm^{-1}): 3021(m), 2927(m), 2811(m), 1634(m), 1587(m), 1494(m), 1340(s); ^{1}H NMR (400 MHz, $CDCl_3$): δ = 9.21 (dd, 1H, *J* = 4 and 4 Hz), 8.82 (d, 2H, *J* = 8 Hz), 8.38 (d, 1H, *J* = 8 Hz), 8.28 (dd, 1H, *J* = 8 and 8 Hz), 8.20 (d, 2H, *J* = 8 Hz), 8.07 (d, 1H, *J* = 8 Hz), 7.54-7.57 (m, 1H); Anal. Calc for $C_{13}H_{19}N_3$ (207.23); C, 75.35; H, 4.38; N, 20.28. Found: C, 75.47; H, 4.46; N, 20.41 %.

General procedure for preparation of neutral napthyridine complexes (1-3)

A mixture of metal precursor $[(arene)MCl_2]_2$ (arene = *p*-cymene, Cp*; M = Ru, Rh and Ir) (0.1 mmol) and ligand 2-(1,8-napthyridin-2-yl)phenol (PHNp) (0.2 mmol) were dissolved in dichloromethane and the reaction mixture was stirred overnight at room temperature. This solution was then filtered over celite and the solvent was evaporated under reduced pressure to afford yellow solid which was washed with diethyl ether (2 x 10 mL) and air dried (Scheme 2).

[(p-cymene)Ru(PHNp)Cl$_2$] (1)

Yield: 69 mg (75%); IR (KBr, cm^{-1}): 3411(b), 3056(m), 1611(m), 1585(m), 1548(m), 1508(m), 1473(m), 1249(m), 1155(s); ^{1}H NMR (400 MHz, DMSO-d_6): δ = 14.92 (s, 1H, OH), 8.89 (d, 1H, *J* = 4 Hz), 8.48 (d, 1H, *J* = 8 Hz), 8.31 (t, 2H, *J* = 8 Hz), 8.07 (d, 1H, *J* = 8 Hz), 7.47-7.50 (m, 1H), 7.22 (t, 1H, *J* = 8 Hz), 6.77-6.82 (m, 2H), 5.61 (d, 2H, *J* = 4 Hz, $CH_{(p\text{-cym})}$), 5.57 (d, 2H, *J* = 8 Hz, $CH_{(p\text{-cym})}$), 2.61 (sept, 1H, $CH_{(p\text{-cym})}$), 1.86 (s, 3H, $CH_{(p\text{-cym})}$), 0.98 (d, 6H, *J* = 8 Hz, $CH_{(p\text{-cym})}$); ^{13}C NMR (100 MHz, DMSO-d_6): δ (ppm) = 160.60, 160.29, 155.19, 149.35, 138.65,

135.10, 133.83, 128.16, 121.69, 121.11, 119.92, 118.16, (C-PHNp), 105.51, 103.91, 87.71, 84.21, 30.31, 23.81, 17.41 (C-*p*-cym); ESI-MS (m/z) [Found (Calcd)]: [456.96 (457.08)] [M-Cl-HCl]$^{+}$; Anal. Calc for $C_{24}H_{24}Cl_2N_2ORu$ (528.43); C, 54.55; H, 4.58; N, 5.30. Found: C, 54.64; H, 4.67; N, 5.39 %.

[Cp*Rh(PHNp)Cl$_2$] (2)

Yield: 82 mg (77%); IR (KBr, cm^{-1}): 3434(b), 2137(m), 1608(m), 1503(m), 1475(m), 1384(m), 1137(m); ^{1}H NMR (400 MHz, DMSO-d$_6$): δ = 15.12 (s, 1H, OH), 9.10 (d, 1H, *J* = 4 Hz), 8.68 (d, 1H, *J* = 8 Hz), 8.51 (d, 2H, *J* = 8 Hz), 8.26 (d, 2H, *J* = 4 Hz), 7.67-7.70 (m, 1H), 7.42 (t, 1H, *J* = 8 Hz), 6.97-7.02 (m, 1H), 1.60 (s, 15H, $CH_{(Cp^*)}$); ^{13}C NMR (100 MHz, DMSO-d$_6$): δ = 160.61, 160.29, 154.49, 152.35, 139.65, 137.30, 132.83, 128.16, 122.69, 121.11, 118.92, 118.83, 118.18 (C-PHNp), 98.68 (Cp^*_{ipso}), 8.51 (Cp^*_{Me}); ESI-MS (m/z) [Found (Calcd)]: [459.02 (459.09)] [M-Cl-HCl]$^{+}$; Anal. Calc for $C_{24}H_{25}Cl_2N_2ORh$ (531.27); C, 54.26; H, 4.74; N, 5.27. Found: C, 54.37; H, 4.87; N, 5.41 %.

[Cp*Ir(PHNp)Cl$_2$] (3)

Yield: 98 mg (78%); IR (KBr, cm^{-1}): 3401(b), 2918(w), 2150(m), 1632(m), 1608(m), 1503(m), 1475(m), 1137(m); ^{1}H NMR (400 MHz, DMSO-d$_6$): δ = 15.12 (s, 1H, OH), 9.10 (dd, 1H, *J* = 4 and 4 Hz), 8.68 (d, 1H, *J* = 8 Hz), 8.51 (t, 2H, *J* = 8 Hz), 8.27 (d, 1H, *J* = 8 Hz), 7.67-7.70 (m, 1H), 7.42 (t, 1H, *J* = 8 Hz), 6.98-7.02 (m, 2H), 1.61 (s, 15H, $CH_{(Cp^*)}$); ^{13}C NMR (100 MHz, DMSO-d$_6$): δ = 160.62, 160.30, 154.49, 152.36, 139.65, 137.30, 132.83, 128.17, 122.69, 121.11, 118.92, 118.26, 118.18 (C-PHNp), 92.01 (Cp^*_{ipso}), 8.17 (Cp^*_{Me}); ESI-MS (m/z) [Found (Calcd)]: [549.10 (549.15)] [M-Cl-HCl]$^{+}$; Anal. Calc for $C_{24}H_{25}Cl_2N_2OIr$ (620.59); C, 46.45; H, 4.06; N, 4.51. Found: C, 46.58; H, 4.14; N, 4.62 %.

General procedure for preparation of cationic napthyridine metal complexes (4-6)

A mixture of metal precursor $[(arene)MCl_2]_2$ (arene = *p*-cymene, Cp*; M = Ru, Rh and Ir) (0.1 mmol) and 2-(1,8-napthyridin-2-yl)aniline (AnNp) were dissolved in dry methanol (5 mL) and stirred at room temperature for 1 hour. Then 4 equivalents of NH_4PF_6 dissolved in dry methanol (2 mL) was added dropwise to the reaction mixture and stirring continued for further 5-6 hours whereupon a yellow solid precipitated out from the reaction mixture. The precipitate was filtered, washed with cold methanol (2 x 5 ml) and diethyl ether (2 x 10 ml) and air dried (Scheme 2).

[(p-cymene)Ru(AnNp)Cl]PF$_6$ (4)

Yield: 101 mg (79%); IR (KBr, cm^{-1}): 3314(m), 3125(m), 1604(m), 1494(w), 1462(w), 1111(m), 842(s); ^{1}H NMR (400 MHz, DMSO-d_6): δ = 9.86 (d, 1H, *J* = 12 Hz), 8.97 (d, 1H, *J* = 4 Hz), 8.70 (d, 1H, *J* = 8 Hz), 8.27 (d, 1H, *J* = 8 Hz), 8.00 (d, 1H, *J* = 4 Hz), 7.86 (t, 1H, *J* = 8 Hz), 7.51-7.57 (m, 2H), 7.31 (t, 2H, *J* = 8 Hz), 5.99 (dd, 2H, *J* = 4 and 4 Hz, $CH_{(p\text{-cym})}$), 5.59 (d, 1H, *J* = 8.0 Hz, $CH_{(p\text{-cym})}$), 5.54 (d, 1H, *J* = 8 Hz, $CH_{(p\text{-cym})}$), 2.19 (sept, 1H, $CH_{(p\text{-cym})}$), 1.98 (s, 3H, $CH_{(p\text{-cym})}$), 0.98 (d, 3H, *J* = 8 Hz, $CH_{(p\text{-cym})}$), 0.89 (d, 3H, *J* = 4 Hz, $CH_{(p\text{-cym})}$); ^{13}C NMR (100 MHz, DMSO-d_6): δ = 161.78, 158.61, 155.19, 148.13, 138.12, 137.32, 134.18, 129.14, 123.41, 120.05, 119.18, 117.16, (C-AnNp), 106.14, 103.41, 89.51, 87.11, 85.22, 30.71, 23.81, 20.21, 16.41 (C-*p*-cym); ESI-MS (m/z) [Found (Calcd)]: [492.06 (492.07)] $[M\text{-}PF_6]^+$, ESI-MS (m/z) [Found (Calcd)]: [456.0 (456.10)] $[M\text{-}PF_6\text{-}HCl]^+$; Anal. Calc for $C_{24}H_{25}ClN_3F_6PRu$ (636.96); C, 45.25; H, 3.96; N, 6.60. Found: C, 45.38; H, 4.07; N, 6.71 %.

[Cp*Rh(AnNp)Cl]PF$_6$ (5)

Yield: 93 mg (72%); IR (KBr, cm^{-1}): 3269(w), 2923(w), 1606(m), 1491(w), 1462(w), 843(s); ^{1}H NMR (400 MHz, DMSO-d_6): δ = 9.23 (d, 1H, *J* = 4 Hz), 8.81 (d, 1H, *J* = 8 Hz), 8.63 (d, 1H, *J* =

8 Hz), 8.25 (d, 1H, *J* = 8 Hz), 7.93 (d, 1H, *J* = 8 Hz), 7.77-7.80 (m, 1H), 7.65 (t, 1H, *J* = 4 Hz), 7.47-7.54 (m, 2H), 7.40 (t, 1H, *J* = 8 Hz), 6.71 (d, 1H, *J* = 4 Hz), 1.34 (s, 15H, $CH_{(Cp^*)}$); ^{13}C NMR (100 MHz, DMSO-d_6): δ = 161.34, 157.13, 153.61, 142.01, 140.24, 139.21, 135.47, 133.45, 126.14, 124.16, 123.12, 120.33, 118.23 (C-AnNp), 89.38 (Cp^*_{ipso}), 8.13 (Cp^*_{Me}); ESI-MS (m/z) [Found (Calcd)]: [494.05 (494.08)] $[M\text{-}PF_6]^+$, ESI-MS (m/z) [Found (Calcd)]: [458.06 (458.11)] $[M\text{-}PF_6\text{-}HCl]^+$; Anal. Calc for $C_{24}H_{26}ClN_3F_6PRh$ (639.80); C, 45.05; H, 4.10; N, 6.57. Found: C, 45.15; H, 4.21; N, 6.63 %.

[Cp*Ir(AnNp)Cl]PF$_6$ (6)

Yield: 110 mg (75%); IR (KBr, cm^{-1}): 3316(w), 3254(w), 3065(w), 2923(w), 1606(m), 1462(w), 1154(w), 842(s); ^1H NMR (400 MHz, $CDCl_3$): δ = 9.34 (d, 1H, *J* = 12 Hz), 8.85 (d, 1H, *J* = 8 Hz), 8.49 (d, 1H, *J* = 8 Hz), 8.18 (d, 1H, *J* = 4 Hz), 8.10 (d, 1H, *J* = 8 Hz), 8.01 (d, 1H, *J* = 8 Hz), 7.80 (d, 1H, *J* = 8 Hz), 7.57 (t, 1H, *J* = 4 Hz), 7.34 (t, 1H, *J* = 8 Hz), 7.23 (d, 1H, *J* = 4 Hz), 6.69 (d, 1H, *J* = 12 Hz), 1.39 (s, 15H, $CH_{(Cp^*)}$); ^{13}C NMR (100 MHz, DMSO-d_6): δ = 160.04, 153.63, 152.89, 142.01, 141.33, 137.57, 131.89, 131.45, 125.84, 123.78, 123.62, 123.36, 119.22 (C-AnNp), 86.38 (Cp^*_{ipso}), 8.07 (Cp^*_{Me}); ESI-MS (m/z) [Found (Calcd)]: [584.07 (584.14)] $[M\text{-}PF_6]^+$, ESI-MS (m/z) [Found (Calcd)]: [548.15 (548.16)] $[M\text{-}PF_6\text{-}HCl]^+$; Anal. Calc for $C_{24}H_{26}ClN_3F_6PIr$ (729.11); C, 39.54; H, 3.59; N, 5.76. Found: C, 39.66; H, 3.68; N, 5.82 %.

General procedure for preparation of neutral napthyridine metal complexes (7-9)

A mixture of metal precursor $[(arene)MCl_2]_2$ (arene = *p*-cymene, Cp*; M = Ru, Rh and Ir) (0.1 mmol) and ligand 2-(pyridine-4-yl)-1,8-napthyridine (PyNp) (0.2 mmol) were dissolved in dry methanol (5 mL) and stirred at room temperature for 6 hours. A yellow compound precipitated out from the reaction mixture. The precipitate was collected washed with cold methanol (2 x 5 mL) and diethyl ether (3 x 10 mL) and air dried (Scheme 2).

[(p-cymene)Ru(PyNp)Cl$_2$] (7)

Yield: 72 mg (70%); IR (KBr, cm^{-1}): 2965(m), 2870(m), 1637(m), 1615(m), 1384(w), 1124(m); ^{1}H NMR (400 MHz, $CDCl_3$): δ = 9.14 (s, 3H), 8.35 (d, 1H, *J* = 8 Hz), 8.24 (d, 1H, *J* = 8 Hz), 8.08 (d, 2H, *J* = 8 Hz), 7.95 (d, 1H, *J* = 8 Hz), 7.53-7.57 (m, 1H), 5.45 (d, 2H, *J* = 4 Hz, $CH_{(p\text{-cym})}$), 5.22 (d, 2H, *J* = 4 Hz $CH_{(p\text{-cym})}$), 2.94 (sept, 1H, $CH_{(p\text{-cym})}$), 2.06 (s, 3H, $CH_{(p\text{-cym})}$), 1.28 (d, 6H, *J* = 8 Hz, $CH_{(p\text{-cym})}$); ^{13}C NMR (100 MHz, $CDCl_3$): δ = 155.78, 154.16, 153.19, 148.23, 139.12, 136.21, 135.11, 130.14, 128.06, 123.05, 119.18, 118.16, (C-PyNp), 106.18, 103.41, 90.13, 88.41, 30.20, 21.84, 17.80 (C-*p*-cym); ESI-MS (m/z) [Found (Calcd)]: [478.21 (478.06)] [M-Cl]$^+$, ESI-MS (m/z) [Found (Calcd)]: [442.15 (443.09)] [M-2Cl]$^+$; Anal. Calc for $C_{23}H_{23}Cl_2N_3Ru$ (513.42); C, 53.80; H, 4.52; N, 8.18. Found: C, 53.93; H, 4.63; N, 8.29 %.

[Cp*Rh(PyNp)Cl$_2$] (8)

Yield: 92 mg (89%); IR (KBr, cm^{-1}): 2985(m), 2860(m), 1635(m), 1609(m), 1378(w), 1127(m); ^{1}H NMR (400 MHz, $CDCl_3$): δ = 9.19 (s, 1H), 9.15 (d, 2H, *J* = 4 Hz), 8.45 (d, 1H, *J* = 8 Hz), 8.31 (dd, 1H, *J* = 4 and 4 Hz), 8.21 (d, 1H, *J* = 8 Hz), 8.04 (d, 2H, *J* = 8 Hz), 7.56-7.59 (m, 1H), 1.63 (s, 15H, $CH_{(Cp^*)}$); ^{13}C NMR (100 MHz, $CDCl_3$): δ = 156.31, 155.42, 154.34, 153.18, 148.33, 139.24, 137.14, 123.43, 123.35, 123.07, 118.14 (C-PyNp), 87.12 (Cp^*_{ipso}), 8.63 (Cp^*_{Me}); ESI-MS (m/z) [Found (Calcd)]: [480.07 (480.15)] [M-Cl]$^+$, ESI-MS (m/z) [Found (Calcd)]: [444.16 (445.10)] [M-2Cl]$^+$; Anal. Calc for $C_{23}H_{24}Cl_2N_3Rh$ (516.26); C, 53.51; H, 4.69; N, 8.14. Found: C, 53.62; H, 4.76; N, 8.23 %.

[Cp*Ir(PyNp)Cl$_2$] (9)

Yield: 86 mg (71%); IR (KBr, cm^{-1}): 2991(m), 2875(m), 1631(m), 1611(m), 1374(w), 1125(m); ^{1}H NMR (400 MHz, $CDCl_3$): δ = 9.20 (s, 1H), 9.13 (d, 2H, *J* = 8 Hz), 8.45 (d, 1H, *J* = 8 Hz), 8.31 (dd, 1H, *J* = 4 and 4 Hz), 8.19 (d, 2H, *J* = 4 Hz), 8.06 (d, 1H, *J* = 8 Hz), 7.57-7.60 (m, 1H),

1.58 (s, 15H, $CH_{(Cp^*)}$); ^{13}C NMR (100 MHz, $CDCl_3$): δ = 155.70, 155.59, 154.74, 153.88, 147.30, 139.32, 137.14, 123.56, 123.10, 123.02, 119.83 (C-PyNp), 86.0 (Cp^*_{ipso}), 8.58 (Cp^*_{Me}); ESI-MS (m/z) [Found (Calcd)]: [570.21 (570.12)] $[M\text{-}Cl]^+$, ESI-MS (m/z) [Found (Calcd)]: [534.23 (535.15)] $[M\text{-}2Cl]^+$; Anal. Calc for $C_{23}H_{24}Cl_2N_3Ir$ (605.07); C, 45.62; H, 3.99; N, 6.94. Found: C, 45.79; H, 4.08; N, 7.05 %.

Results and discussion

Synthesis of napthyridine ligands and metal complexes

The napthyridine ligands were synthesized according to Friedländer condensation reaction and the napthyridine metal complexes (**1**-**9**) were synthesized by the reaction of metal precursors with respective napthyridine ligands. At first the reaction of PHNp with metal precursor was carried out using triethylamine as base with an aim of deprotonating phenolic hydrogen which would result in formation of NO chelated complex but no deprotonation occurred as evidenced from the ^1H NMR spectra of the complexes which showed the presence of phenolic proton. So the reaction was carried out without using triethylamine and which resulted in formation of the same compounds. X-ray studies revealed that the PHNp ligand coordinated metal in a monodentate manner through napthyridine nitrogen. Reaction of AnNp with precursor afforded mononuclear bidentate chelated complexes. Surprisingly substituting 4-pyridyl group at the 2-position of 1,8-napthyridine in PyNp yielded complexes where PyNp is coordinated to metal through pyridine nitrogen rather than napthyridine nitrogen as in case of PHNp complexes. The three-napthyridine ligands used in this work exhibited interesting coordination modes. Complexes of PHNp and PyNp ligands were isolated as neutral complexes whereas with AnNp ligand, complexes were isolated as ionic salts with PF_6 counter ion. The napthyridine ligands and metal complexes were obtained in good yields. These complexes are soluble in organic solvents

such as chloroform, dichloromethane, acetonitrile and DMSO but insoluble in diethyl ether and hexane. The napthyridine ligands and the napthyridine metal complexes were characterized spectroscopically and the molecular structures of some of the complexes were established by single crystal X-ray analysis.

Spectroscopic characterization of napthyridine ligands

The infrared spectra of PHNp and AnNp ligands exhibited stretching frequencies for OH at 3521 cm^{-1} and for the NH_2 group at 3402 and 3293 cm^{-1}. The C=N and C=C stretching frequencies of the napthyridine ligands were observed in the range of 1450-1650 cm^{-1}. The proton NMR spectra of the napthyridine ligands displayed signals in the range of 6.46-9.21 ppm for the protons of the napthyridine moiety and substituted rings. In addition to these resonances the PHNp ligand displayed a singlet at 14.7 ppm for the phenolic proton and the AnNp ligand exhibited a broad singlet for the NH_2 proton at 7.34 ppm respectively. The respective ^1H NMR spectra of the napthyridine ligands are presented in the SI.

Spectroscopic characterization of napthyridine metal complexes

IR studies of metal complexes

The IR spectra of the metal complexes suggest the coordination of the napthyridine ligands to the metal atom. The presence of a broad band for complexes (**1**-**3**) in the lower frequency region around 3401-3434 cm^{-1} for the phenolic OH group suggests that the phenolic group is not involved in coordination to the metal center. This was further supported by NMR and single crystal analysis. Complexes (**4**-**6**) displayed characteristic stretching frequencies for NH_2 group at lower frequency region around 3125-3326 cm^{-1} as compared to the free ligand at 3402 and 3293 cm^{-1}. This shift to lower frequency suggests the coordination of the NH_2 group. Further the C=N stretching frequencies of the complexes decreases slightly and was observed in

the range of 1603-1615 cm^{-1} as compared to the free ligand which suggest the coordination of the napthyridine and pyridine nitrogen's. In addition to these bands a sharp band for the cationic complexes (**4**-**6**) was observed around 842-843 cm^{-1} attributed to the P-F stretching frequency of the counter ion [23].

^{1}H NMR studies of metal complexes

The ^{1}H NMR spectra of the metal complexes further support the formation of the complexes. The resulting spectra are depicted in the supplementary information and ensuing data are summarized in the experimental section. The metal complexes exhibited signals associated with the ligand protons and signals due to *p*-cymene and Cp* ring protons. The signals associated with the napthyridine and substituted ring protons were observed in the downfield region around 6.65-9.86 ppm. This shifting of the ligand resonances indicates the coordination of the napthyridine ligands to the metal atom. Also the appearance of the phenolic proton signals in complexes (**1**-**3**) around 14.9-15.1 ppm confirms that the phenolic OH group is not involved in coordination to the metal atom. Further confirmation of the binding of napthyridine ligands was confirmed by the appearance of the *p*-cymene and Cp* ring proton signals. The aromatic protons of the *p*-cymene ligand consisted of doublets around 5.22-5.99 ppm. The isopropyl group of the *p*-cymene ligand displayed doublet for complexes (**1** and **7**) whereas for complex (**4**) it showed two doublets around 0.89-1.28 ppm. The methyl and methine protons of the *p*-cymene ligand were observed as a singlet around 1.98-2.07 ppm and septet around 2.19-2.94 ppm. The methyl protons of the Cp* moiety was observed as a singlet around 1.34-1.61 ppm.

^{13}C NMR studies of metal complexes

The ^{13}C NMR spectra further justify the formation of the complexes. The ^{13}C NMR spectra of the complexes displayed signals associated with the napthyridine carbons and the

appearance of the *p*-cymene moiety carbons, methyl carbon of Cp* and ring carbon of Cp* confirms the formation of these complexes. In the ^{13}C NMR spectra of the complexes the carbon resonances associated with the napthyridine ligand were observed in the region around 118-161 ppm. The aromatic carbon resonances of the *p*-cymene ligand were observed in the region around 84-106 ppm. The methine, isopropyl and methyl carbon resonances of the *p*-cymene moiety were observed in the region around 16-31 ppm. In addition to these carbon resonances the ring carbons of the Cp* ligand displayed signal around 86.0-98.6 ppm and the signal for the methyl protons of the Cp* moiety was observed around 8.07-8.63 ppm. Overall results from NMR spectral studies strongly support the formation of the metal complexes.

Mass spectral studies of metal complexes

The composition and formation of napthyridine metal complexes (**1**-**9**) have further been justified by ESI-mass spectral studies. The mass spectra of the complexes are presented in the supplementary information and the values are listed in the experimental section (2.5). The mass spectra of the complexes (**1**–**3**) displayed their molecular ion peaks at m/z: 456.96, m/z: 459.02 and m/z: 549.10 corresponding to $[M\text{-}Cl\text{-}HCl]^+$ ion. Complexes (**4**-**6**) displayed their molecular ion peaks at m/z: 492.06, m/z: 494.05 and m/z: 584.07 which corresponds to $[M\text{-}PF_6]^+$ ion peak. Also peaks were observed at m/z: 456.0, m/z: 458.06 and m/z: 548.15 which is due to $[M\text{-}PF_6\text{-}HCl]^+$ ion. Similarly complexes (**7**-**9**) displayed peaks at m/z: 478.21, m/z: 480.15 and m/z: 570.21 which is due to the loss of one chloride $[M\text{-}Cl]^+$ ion and also it exhibited peaks at m/z: 442.15, m/z: 444.16 and m/z: 534.23 which is due to the loss of both the chloride $[M\text{-}2Cl]^+$ ion.

Description of the crystal structures of complexes

Apart from spectroscopic analysis, the molecular structures of some of the respective complexes were established by single crystal X-ray analysis. Our attempt to isolate the single

crystal for all the complexes was unsuccessful; however we obtained single crystals for the PHNp ligand and complexes **3**, **4**, **5**, **8** and **9** respectively. By carrying out the single crystal analyses we were able to confirm the various coordination modes of the napthyridine ligand and the geometry of the complexes. The data and molecular structure of complexes **3** and **9** presented here is to only confirm the structure and composition of the molecule. The ORTEP plot of PHNp and the complexes along with atom numbering scheme are shown in (Figures 1-5) respectively. The summary of the crystal data including data collection and structure refinement parameters are summarized in Table 1 and geometrical parameters including bond lengths, bond angles and metal atom involving ring centroid values are listed in Table 2. The molecular structure of PHNp ligand is shown in (Figure 1). Complexes (**1**-**3**) and (**7**-**9**) have the neutral species with formula [(arene)M(PHNp)Cl_2] and [(arene)M(PyNp)Cl_2] [(arene) = *p*-cymene, M = Ru (**1**), (**7**); Cp*, M = Rh (**2**), (**8**) and Ir (**3**), (**9**)]. Complexes (**4**-**6**) have the cationic species with general formula [(arene)M(AnNp)Cl] [(arene) = *p*-cymene, M = Ru (**4**); Cp*, M = Rh (**5**) and Ir (**6**)] and counter anion PF_6. These complexes adopts a familiar three legged piano-stool geometry around the metal center with coordination sites occupied by arene/Cp* ring (arene = *p*-cymene and Cp*) in a η^6/η^5 manner, nitrogen donor atoms from napthyridine ligand and terminal chloride. The geometry at the metal atom is pseudo-octahedral wherein the polycyclic arene ligand acts as seat and napthyridine ligand and terminal chloride form the legs. In complex (**3**) iridium metal is coordinated through Cp* ring, PHNp ligand in a monodentate fashion coordinating iridium through napthyridine nitrogen (N1) and two chlorides thus possessing a three-legged piano-stool structure (Figure 2). In complexes **4** and **5** the metal is coordinated through *p*-cymene and Cp* ring, AnNp ligand in a bidentate manner and one chloride. The AnNp ligand acts as a chelating ligand coordinating metal through aniline nitrogen N(1) and napthyridine nitrogen (N2) forming

a six membered metallacycle (Figure 3). The napthyridine nitrogen N(3) is not involved in coordination. Similarly in complex **8** the metal is coordinated through two chloride's, Cp* moiety and PyNp ligand wherein it acted as a neutral monodentate ligand coordinating rhodium through pyridine nitrogen (N1) (Figure 4 and 5). The distance between the metal to centroid of the arene/Cp* ring are {1.775 (**3**), 1.799 (**4**), 1.803 (**5**) and 1.773 (**8**) and 1.778 (**9**) Å}. The Metal to nitrogen (M-N) bond distances in these complexes is found to be in the range of 2.11-2.17 Å which are in close agreement for reported complexes with napthyridine ligands (Table 2) [10, 13]. It is to be noted that in complexes (**4** and **5**) the M-N bond distance {2.143(3) and 2.138(2), Å} from aniline N(1) is comparatively shorter than the napthyridine N(2) nitrogen-metal distances {2.164(3) and 2.179(3) Å}. The M-Cl bond lengths in these complexes shows no significant differences and was found to be in the range of 2.405-2.447 Å which are comparable with earlier reported complexes [24]. The bite angle values in in these napthyridine complexes were observed in the range of 80.0-91.3° which are consistent with the piano stool arrangement of various groups around the metal center (Table 2) [25, 26].

Further from the crystal packing diagram it was observed that complex (**4**) formed a dimeric unit via intermolecular van der Waal N-H·····Cl (2.647 Å) interaction between the terminal chloride and amino hydrogen (Figure 6). Also in complex (**5**) two different types of weak intermolecular van der Waal N-H·····Cl (2.548 Å) between chloride and amino group of AnNp and C-H·····Cl (2.815 Å) interactions between chloride and napthyridine hydrogen was observed (Figure 7). Interestingly the crystal packing in complex (**8**) formed a dimeric unit via intermolecular van der Waal C-H·····Cl (2.723 and 2.809 Å) interaction between the chloride ion and H-atom from napthyridine and pyridine of PyNp (Figure 8). These weak interactions play a significant role in the formation of supramolecular motifs with interesting features.

Chemosensitivity studies

The response of HCT-116 and MIA-PaCa-2 cells to the napthyridine ligands and the respective metal complexes (**1**-**9**) are presented in Table 3. PHNp ligand was found to be moderately active against both HCT-116 and MIA-PaCa-2 cell lines with IC_{50} values of 39.90±1.60 and 62.48±6.28 μM respectively. In contrast, both AnNp and PyNp were found to be inactive with IC_{50} value > 100 μM against both the cell lines. Upon complexation of napthyridine ligands complexes (**1**-**3**) of PHNp ligand displayed less activity whereas PyNp complexes did not display any cytotoxicity and iridium complex (**6**) with AnNp ligand possessed the highest activity against HCT-116 cells. Complexes (**1**-**3**) were found to be active against HCT-116 cell line with IC_{50} value in the range of 37.79±4.90 to 82.09±3.55 μM as compared to PHNp ligand whose IC_{50} value is 39.90±1.60 μM. Against the Mia-PaCa-2 cell line, complex (**2**) was the most active with an IC_{50} of 25.13±6.07 μM. Complexes (**3**) and (**6**) were moderately active against the MIA-PaCa-2 cell line with IC_{50} values of 52.13±12.28 and 82.09±2.55 μM. Differences between the response of HCT116 and Mia-PaCa-2 cells exist suggesting that these complexes are targeting inherent biochemical differences between these cells as opposed to having general cytotoxic properties. However, all the compounds were found to be less cytotoxic as compared to cisplatin whose IC_{50} value is 2.78 μM. In contrast to cisplatin however, none of the novel compounds tested exhibited a cytotoxic effect on the non-cancer ARPE-19 cell line (IC_{50} values were > 100 μM). The selectivity ratio for cisplatin (defined as the IC_{50} of ARPE-19 divided by the IC_{50} of cancer cell lines) was 1.23 for HCT-116 cells whereas for complex (**3**), the selectivity index was >2.64. Similar values for the selectivity index were obtained for other complexes tested suggesting that whilst potency is reduced compared to cisplatin, selectivity for cancer cells *in vitro* under identical experimental conditions is enhanced.

Conclusion

In this work, we report the coordination chemistry of 2-substituted-1,8-naphthyridine ligands towards ruthenium, rhodium and iridium half-sandwich complexes. Complexes of PHNp and PyNp were isolated as neutral complexes whereas AnNp complexes were isolated as ionic salts with PF_6 counter anion. The molecular structures of neutral complexes revealed that PHNp and PyNp ligands acted as monodentate ligand coordinating metal through napthyridine nitrogen (N1) and pyridine nitrogen N(1). Whereas the X-ray structures of cationic complexes with AnNp ligand showed that it behaved as neutral chelating ligand coordinating metal atom in a bidentate NN´ fashion through aniline nitrogen N(1) and napthyridine nitrogen (N2) forming a six-membered chelated ring. Chemosensitivity activity of the complexes carried out against HCT-116 and MIA-PaCa-2cancer cell lines showed that PHNp and its complexes are cytotoxic; however iridium-based AnNp complex possessed the highest activity among all other napthyridine complexes. The work presented here exhibits interesting coordination modes of the 2-substituted-1,8-napthyridine ligands that have cytotoxic activity against cancer cells *in vitro*. Whilst the potency of these compounds is less than cisplatin, there is evidence to suggest that these complexes have greater selectivity for cancer as opposed to non-cancer cells *in vitro* than cisplatin and therefore representing promising compounds for further development and evaluation.

Acknowledgements

Sanjay Adhikari thanks, UGC, New Delhi, India for providing financial assistance in the form of university fellowship (UGC-Non-Net). We thank DST-PURSE SCXRD, NEHU-SAIF, Shillong, India for providing Single crystal X-ray analysis and other spectral studies.

Supplementary material

CCDC **1568178** (**4**), **1568179** (**5**), **1568180** (**8**), **1568181** (**PHNp**), contains the supplementary crystallographic data for this paper. These data can be obtained free of charge via www.ccdc.cam.ac.uk/data_request/cif, by e-mailing data_request@ccdc.cam.ac.uk, or by contacting The Cambridge Crystallographic Data Centre, 12, Union Road, Cambridge CB2 1EZ, UK; Fax: +44 1223 336033.

References

[1] B. Therrien, Coord. Chem. Rev. 253 (2009) 493.

[2] S. Y. Mudi, T. M. Usman, S. Ibrahim, Am. J. Chem. Appl. 2 (2015) 151.

[3] G. Gasser, I. Ott, N. M-Nolte, J. Med. Chem. 54 (2011) 3.

[4] A. A. Nazarov, C. G. Hartinger, P. J. Dyson, J. Organomet. Chem. 751 (2014) 251.

[5] (a) H. Chen, J. A. Parkinson, S. Parsons, R. A. Coxall, R. O. Gould, P. J. Sadler, J. Am. Chem. Soc. 124 (2002) 3064, (b) R. E. Morris, R. E. Aird, P. S. Murdoch, H. Chen, J. Cummings, N. D. Hughes, S. Parsons, A. Parkin, G. Boyd, D. I. Jodrell, P. J. Sadler, J. Med. Chem. 44 (2001) 3616, (c) R. E. Aird, A. A. Ritchie, M. Muir, R. E. Morris, H. Chen, P. J. Sadler, D. I. Jodrell, Br. J. Cancer, 86 (2002) 1652.

[6] (a) C. S. Allardyce, P. J. Dyson, D. J. Ellis, S. L. Heath, Chem. Comm. (2001) 1396, (b) C. Scolaro, A. Bergamo, L. Brescacin, R. Delfino, M. Cocchietto, G. Laurenczy, T. J. Geldbach, G. Sava, P. J. Dyson, J. Med. Chem. 48 (2005) 4161.

[7] Y. Geldmacher, M. Oleszak, W. S. Sheldrick, Inorg. Chim. Acta, 393 (2012) 84.

[8] O. Prakash, K. N. Sharma, H. Joshi, P. L. Gupta, A. K. Singh, Organometallics, 33 (2014) 2535.

[9] N. Hofmann, L. Ackermann, J. Am. Chem. Soc. 135 (2013) 5877.

[10] T. Suzuki, Inorg. Chim. Acta, 359 (2006) 2431.

[11] S. K. Patra, N. Sadhukhan, J. K. Bera, Inorg. Chem. 45 (2006) 4007.

[12] A. Sinha, M. Majumdar, M. Sarkar, T. Ghatak, J. K. Bera, Organometallics, 32 (2013) 340.

[13] K. T. Prasad, B. Therrien, K. M. Rao, J. Organomet. Chem. 693 (2008) 3049.

[14] D. D. Perrin, W. L. F. Armarego, Purification of Laboratory Chemicals, fourth ed., Butterworths Heinemann, London, 1996.

[15] M. A. Bennett, T. N. Huang, T. W. Matheson, A. K. Smith, S. Ittel, W. Nickerson, Inorg. Synth. 21 (1982) 74.

[16] C. White, A. Yates, P. M. Maitlis, D. M. Heinekey, Inorg. Synth. 29 (2007) 228.

[17] G. M. Sheldrick, Acta Crysat. Sect. A 46 (1990) 467.

[18] G. M. Sheldrick, Acta Cryst. Sect. A 64 (2008) 112.

[19] L. J. Farrugia, J. Appl. Cryst. 32 (1999) 837.

[20] Z. Almodares, S. J. Lucas, B. D. Crossley, A. M. Basri, C. M. Pask, A. J. Hebden, R. M. Phillips, P. C. McGowan, Inorg. Chem. 53 (2014) 727.

[21] S. J. Lucas, R. M. Lord, R. L. Wilson, R. M. Phillips, V. Sridharan, P. C. McGowan, Dalton Trans. 41 (2012) 13800.

[22] Q. Zhao, S. Liu, M. Shi, C. Wang, M. Yu, L. Li, F. Li, T. Yi, C. Huang, Inorg. Chem. 45 (2006) 6152.

[23] S. Adhikari, D. Sutradhar, S. L. Shepherd, R. M. Phillips, A. K. Chandra, K. M. Rao, J. Organomet. Chem. 820 (2016) 70.

[24] A. Pastuszko, K. Niewinna, M. Czyz, A. Jozwiak, M. Malecka, E. Budzisz, J. Organomet. Chem. 745 (2016) 64.

495 [25] C. M. Clavel, E. Paunescu, P. N-Sliwinska, A. W. Griffioen, R. Scopelliti, P. J. Dyson, J.
496 Med. Chem. 57 (2014) 3546.
497 [26] S. Adhikari, W. Kaminsky, M. R. Kollipara, J. Organomet. Chem. 848 (2017) 95.

498

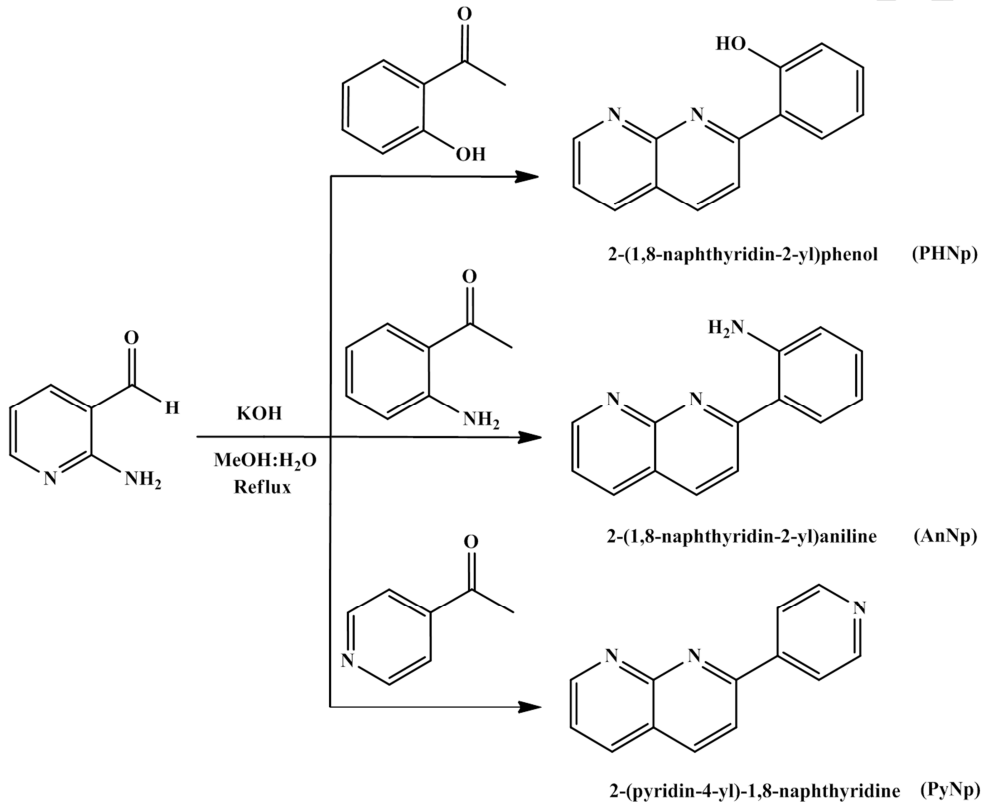

499

500 Scheme 1 Synthetic routes of ligands

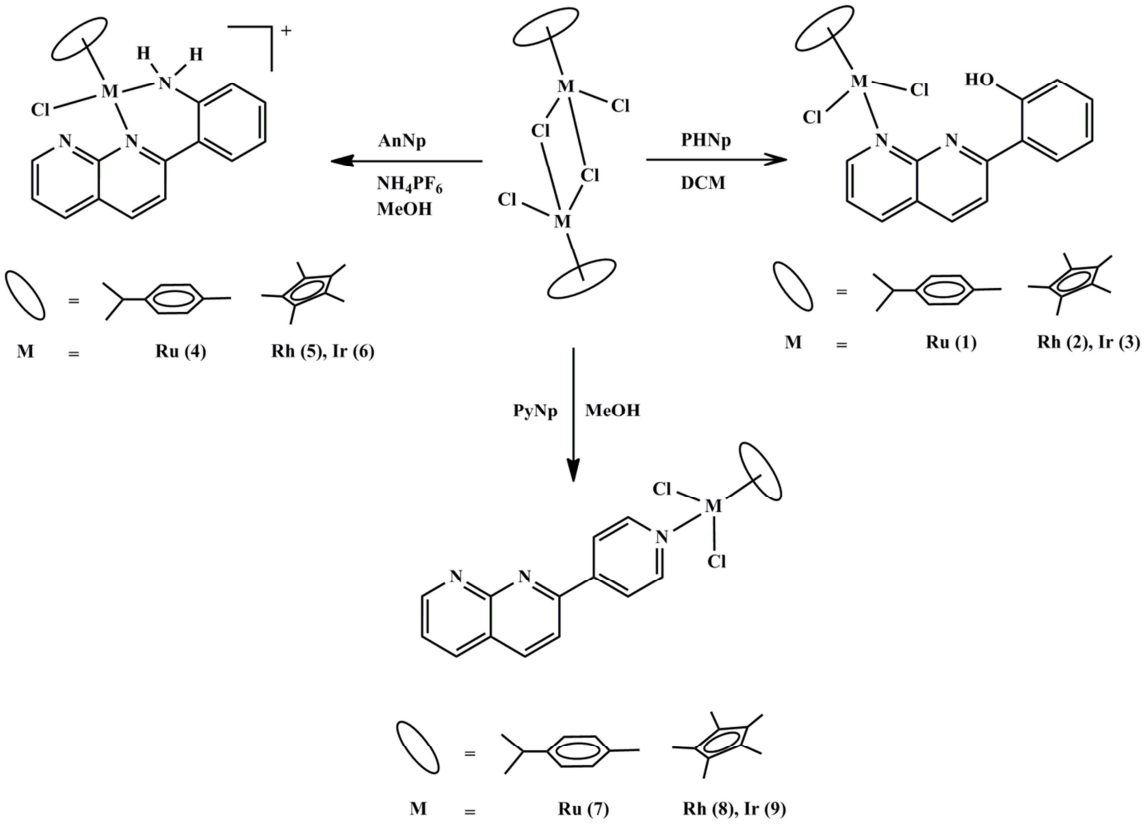

Scheme 2 Synthesis of neutral and cationic napthyridine metal complexes (**1**-**9**)

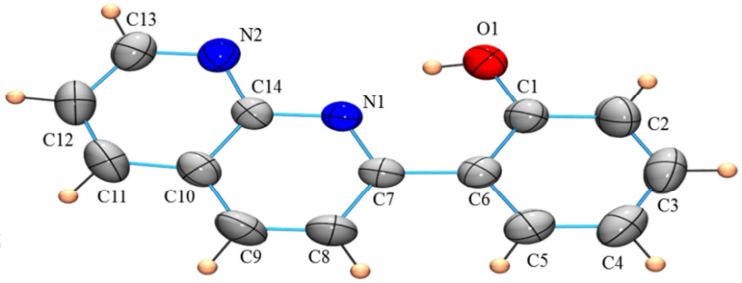

Figure 1 ORTEP plot of PHNp with 50% probability thermal ellipsoids.

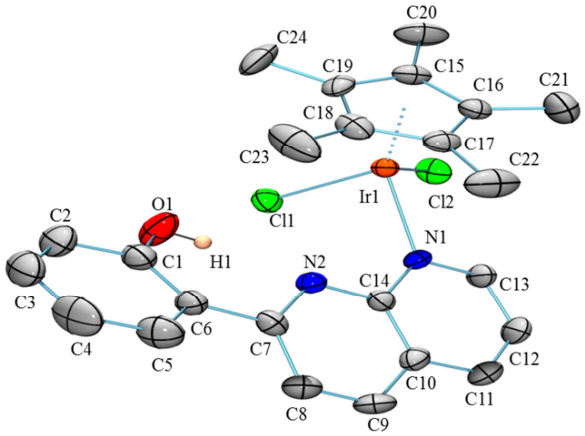

Figure 2 ORTEP plot of complex (**3**) with 50% probability thermal ellipsoids. Hydrogen atoms (except on O1) are omitted for clarity.

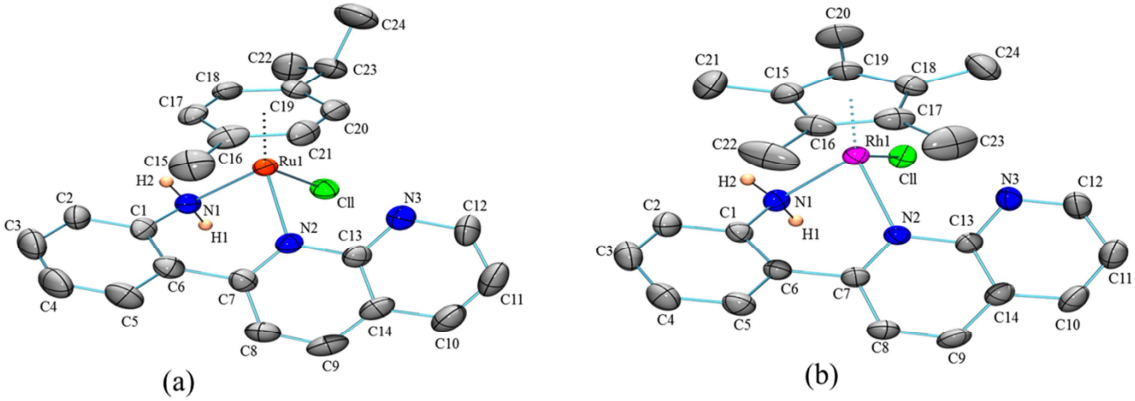

Figure 3 (a) ORTEP plot of complex (**4**) and (b) ORTEP plot of complex (**5**) with 50% probability thermal ellipsoids. Counter anions, hydrogen atoms (except on N1) are omitted for clarity.

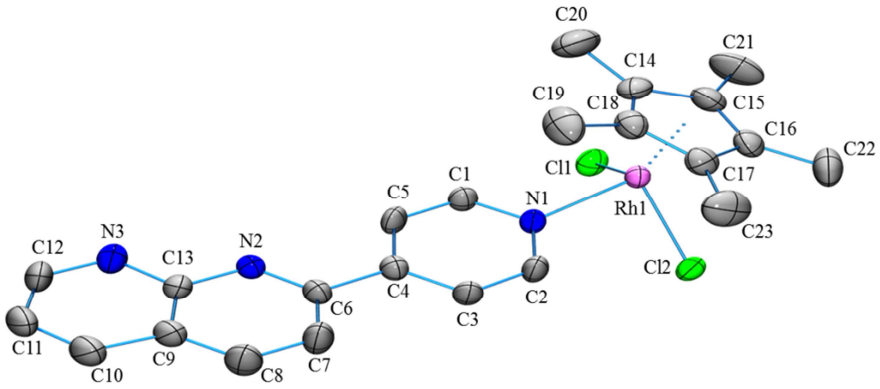

514

515 Figure 4 ORTEP plot of complex (**8**) with 50% probability thermal ellipsoids. Solvent molecules

516 and hydrogen atoms are omitted for clarity.

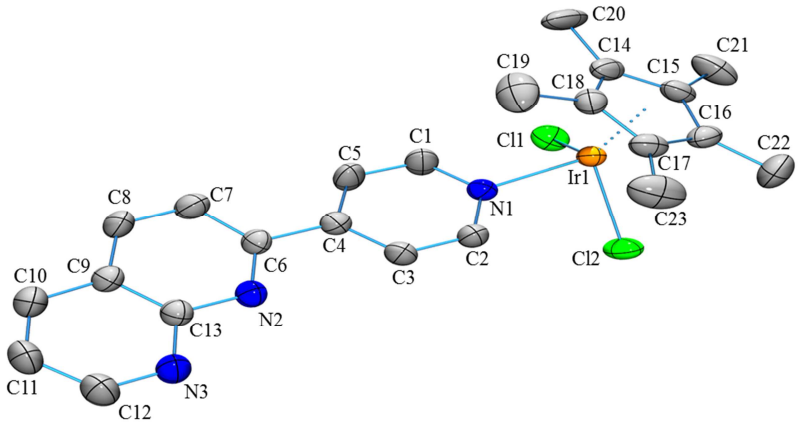

517

518 Figure 5 ORTEP plot of complex (**9**) with 50% probability thermal ellipsoids. Solvent molecule

519 and hydrogen atoms are omitted for clarity.

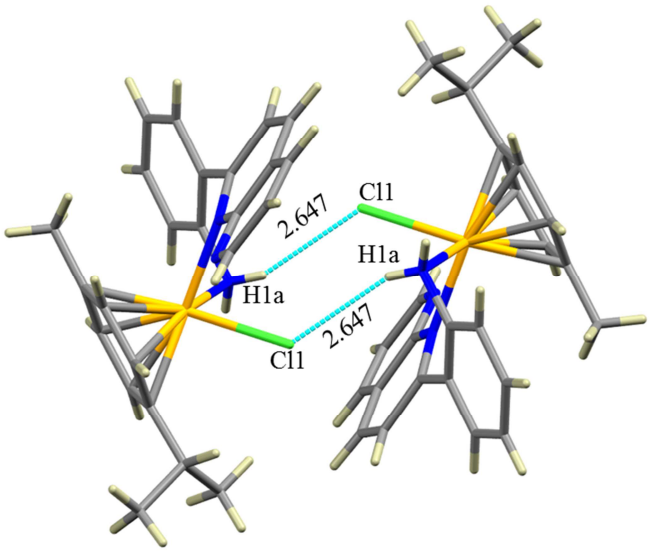

Figure 6 Packing diagram of complex (**4**) showing a dimeric unit formed via intermolecular van der Waal N-H·····Cl (2.647 Å) interaction between the terminal chloride and amino hydrogen.

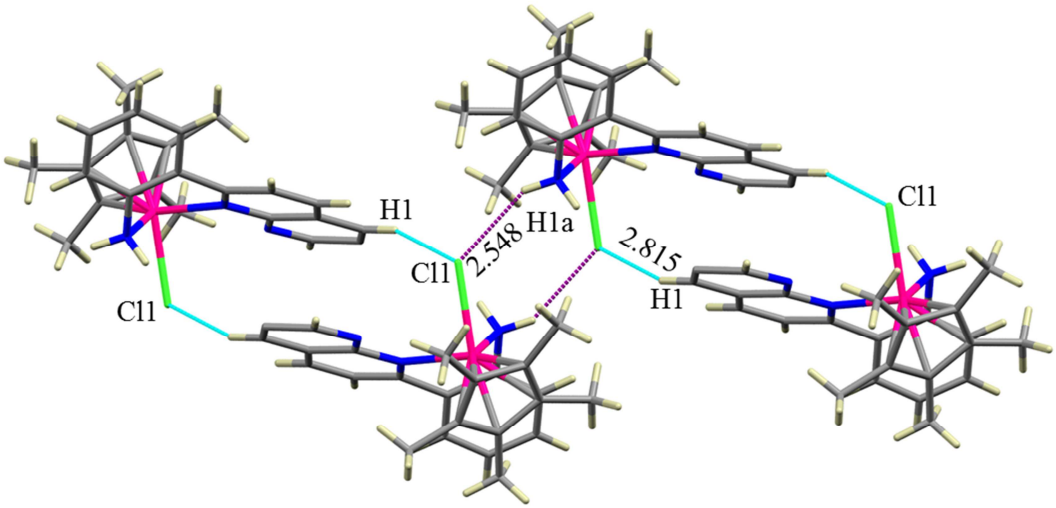

Figure 7 Packing diagram of complex (**5**) showing two different types of weak intermolecular van der Waal N-H·····Cl and C-H·····Cl interactions.

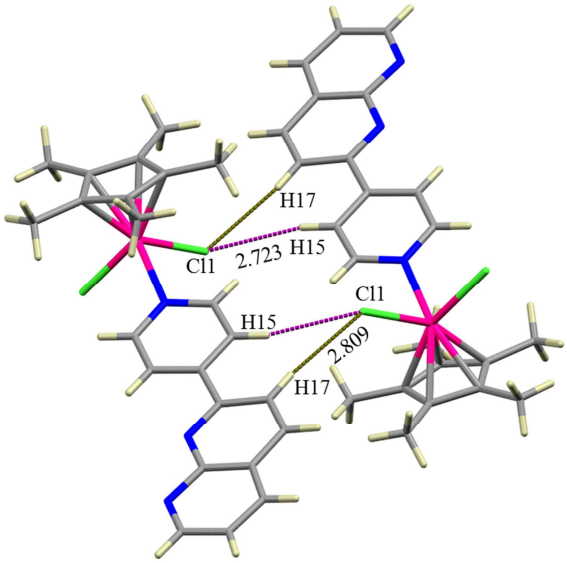

526

527 Figure 8 Crystal packing diagram of complex (**8**) showing a dimeric unit formed via

528 intermolecular van der Waal C-H·····Cl interactions.

529

Table1 Crystal data and structure refinement parameters of complexes

Complexes	PHNp	[**3**]	[**4**] PF_6. CH_2Cl_2	[**5**] PF_6	[**8**] $CHCl_3$	[**9**] $CHCl_3$
Empirical formula	$C_{14}H_{10}N_2O$	$C_{24}H_{25}Cl_2N_2OIr$	$C_{25}H_{27}Cl_3F_6N_5PRu$	$C_{24}H_{25}ClF_6N_3PRh$	$C_{24}H_{25}Cl_5N_3Rh$	$C_{24}H_{25}Cl_5N_3Ir$
Formula weight	222.24	620.56	721.89	638.80	635.63	724.94
Temperature (K)	295(5)	293.6(4)	294(2)	293.6(2)	293.46(16)	295.8(5)
Wavelength (Å)	0.71073	0.71073	0.71073	0.71073	0.71073	0.71073
Crystal system	monoclinic	monoclinic	triclinic	triclinic	monoclinic	orthorhombic
Space group	$P2_1/n$	$P2_1/c$	$P\bar{1}$	$P\bar{1}$	$P2_1/c$	$Pbca$
a (Å)/α (°)	6.7873(9)/90	13.4948(7)/90	10.7040(6)/89.251	10.4457(6)/103.015(5)	14.6829(6)/90	14.5012(7)/90
b (Å)/β (°)	7.4846(8)/91.156(11)	7.9005(4)/100.679(6)	12.2053(7)/72.359(5)	11.3360(6)/109.254(5)	13.1266(5)/104.747	14.1704(9)/90
c (Å)/γ (°)	21.206(3)/90	21.1365(15)/90	13.0455(8)/64.432(5)	11.8077(6)/94.772(4)	14.4475(6)/90	26.0020(10)/90
Volume ($Å^3$)	1077.1(2)	2214.5(2)	1451.22(15)	1267.08(13)	2692.84(19)	5343.1(5)
Z	4	4	2	2	4	11
Density (calc) (Mg/m^{-3})	1.371	1.861	1.652	1.674	1.568	1.802
Absorption coefficient (μ) (mm^{-1})	0.089	0.832	0.931	0.906	1.148	5.516
F(000)	464	1208	724	642	1280	2816
Crystal size (mm^3)	0.25 x 0.23 x 0.21	0.21 x 0.12 x 0.09	0.27 x 0.21 x 0.15	0.25 x 0.15 x 0.07	0.25 x 0.23 x 0.21	0.35 x 0.25 x 0.15
Theta range for data collection	3.844 to 28.941°	3.240 to 29.075°	3.19 to 29.02°	3.332 to 29.115°	3.262 to 28.993°	3.5140 to 28.7290°
Index ranges	-9<=h<=5, -5<=k<=10, -26<=l<=25	-18<=h<=15, -5<=k<=10, -28<=l<=27	-14<=h<=13, -16<=k<=16, -17<=l<=16	-14<=h<=14, -15<=k<=15, -40<=l<16	-20<=h<=18, -11<=k<=17, -19<=l<12	-19<=h<=17, -12<=k<=16, -32<=l<18
Reflections collected	3683	6905	10127	8777	11091	14307
Independent reflections	2370 [R(int) = 0.0209]	4465 [R(int) = 0.0265]	6534 [R(int) = 0.0445]	5707 [R(int) = 0.0267]	6178 [R(int) = 0.0309]	5588 [R(int) = 0.0317]
Completeness to theta = 25.00°	96.2 %	89.5 %	99.5 %	99.5 %	99.3 %	78.7 %
Absorption correction	Semi-empirical from equivalents	Semi-empirical from equivalents	Semi-empirical from equivalents	Semi-empirical from equivalents	Semi-empirical from equivalents	Semi-empirical from equivalents
Max and min transmission	1.0000 and 0.67974	1.0000 and 0.36096	0.8730 and 0.7871	1.0000 and 0.69116	26.37 and 3.26	1.00000 and 0.31067
Refinement method	Full-matrix least-squares on F^2	Full-matrix least-squares on F^2	Full-matrix least-squares on F^2	Full-matrix least-squares on F^2	Full-matrix least-squares on F^2	Full-matrix least-squares on F^2
Data/restraints/parameters	2370/0/154	4465/0/270	6534/5/377	5707/0/325	6178/0/298	6178/0/298
Goodness-of-fit on F^2	1.088	1.013	1.038	1.051	1.061	1.077
Final R indices [I>2sigma(I)]	R1 = 0.0566, wR2 = 0.1361	R1 = 0.0346, wR2 = 0.0699	R1 = 0.0552, wR2 = 0.1360	R1 = 0.0361, wR2 = 0.0895	R1 = 0.0505, wR2 = 0.1047	R1 = 0.0402, wR2 = 0.0781
R indices (all data)	R1 = 0.0871, wR2 = 0.1615	R1 = 0.524, wR2 = 0.0346	R1 = 0.0691, wR2 = 0.1469	R1 = 0.0423, wR2 = 0.0935	R1 = 0.0664, wR2 = 0.1127	R1 = 0.0588, wR2 = 0.0858
Largest diff. peak and hole ($e.Å^{-3}$)	0.193 and -0.148	1.319 and -0.929	0.879 and -0.698	0.650 and -0.539	0.843 and -0.861	1.518 and -1.005
CCDC No.	1568181	----	1568178	1568179	1568180	----

Structures were refined on F_0^2: $wR_2 = [\Sigma[w(F_0^2 - F_c^2)^2] / \Sigma w(F_0^2)^2]^{1/2}$, where $w^{-1} = [\Sigma(F_0^2)+(aP)^2+bP]$ and $P = [\max(F_0^2, 0)+2F_c^2]/3$

532 Table 2 Selected bond lengths (Å) and bond angles (°) of complexes

Complex	**3**	**4**	**5**	**8**	**9**
M(1)-CNT	1.775	1.799	1.803	1.773	1.778
M(1)-N(1)	2.154(4)	2.143(3)	2.138(2)	2.128(3)	2.117(5)
M(1)-N(2)	----	2.164(3)	2.179(3)	2.427(1)	
M(1)-Cl(1)	2.405(1)	2.4165(11)	2.4478(7)	2.405(1)	2.409(2)
M(1)-Cl(2)	2.426(2)	----	----	----	2.404(1)
N(1)-M(1)-N(2)	----	82.29(14)	80.12(8)	----	
N(1)-M(1)-Cl(1)	87.7(1)	82.67(10)	82.90(6)	87.27(8)	87.6(1)
N(2)-M(1)-Cl(1)	----	83.55(10)	91.00(6)	----	----
N(1)-M(1)-Cl(2)	89.0(1)	----	----	89.76(8)	85.9(1)
Cl(1)-M(1)-Cl(2)	85.13(5)	----	----	91.25(4)	89.46(5)

533 CNT represents the centroid of the arene/Cp* ring and M = Ru, Rh and Ir.

534 Table 3 IC_{50} values of napthyridine ligands and complexes (**1**-**9**) along with cisplatin against
535 HCT-116 and MIA-PaCa-2 cancer cell line and non-cancer ARPE-19 cell line. Each value
536 represents the mean ± standard deviation from three independent experiments.

Compounds	IC_{50} (µM)		
	HCT-116	MIA-PaCa-2	ARPE-19
PHNp	39.90±1.64	62.48±6.28	>100
AnNp	>100	>100	>100
PyNp	>100	>100	>100
Complex **1**	82.09±3.54	>100	>100
Complex **2**	61.28±13.8	25.14±6.07	>100
Complex **3**	37.79±4.89	52.13±12.28	>100
Complex **4**	>100	>100	>100
Complex **5**	>100	>100	>100
Complex **6**	31.33±12.92	82.09±2.55	>100
Complex **7**	>100	>100	>100
Complex **8**	>100	>100	>100
Complex **9**	>100	>100	>100
Cisplatin	2.78±1.40	3.15 ± 0.10	3.43±0.48

537 IC_{50} = concentration of the drug required to inhibit the growth of 50% of the cancer cells (µM).

Highlights

- 2-substituted-napthyridine derivatives are synthesized by Friedländer condensation.
- Interesting bonding modes of napthyridine ligands were observed.
- Complexes were cytotoxic against cancer cell lines.